Pergamon

Solid State Communications, Vol. 97, No. 3, pp. 169-174, 1996
Elsevier Science Ltd
Printed in Great Britain
0038-1098/96 $9.50+.00

0038-1098(95)00624-9

RESONANT SPIN-FLIP RAMAN SCATTERING and LOCALIZED EXCITON LUMINESCENCE in SUBMONOLAYER InAs-GaAs STRUCTURES

A.A. Sirenko *) and T. Ruf
Max-Planck Institut für Festkörperforschung, Heisenbergstrasse 1,
D-70569 Stuttgart, Germany
N.N. Ledentsov, A.Yu. Egorov, P.S. Kop'ev, V.M. Ustinov, and A.E. Zhukov.
A.F. Ioffe Physical Technical Institute, Russian Academy of Sciences,
Politekhnicheskaya 26, 194021 St. Petersburg, Russia

(*Received* 27 *August* 1995; *accepted* 18 *September* 1995 *by M. Cardona*)

We report on efficient resonant spin-flip Raman scattering due to localized heavy-hole excitons in single submonolayer InAs insertions in a GaAs matrix. Exciton, heavy-hole and electron g factors are directly measured for samples with different average thicknesses of InAs. The large size uniformity of the InAs islands manifests itself in very narrow heavy- and light-hole exciton photoluminescence peaks which also allow us to measure exciton g factors by magneto-luminescence spectroscopy.

Keywords: A. nanostructures, A. semiconductors, E. inelastic light scattering, E. luminescence.

INTRODUCTION

Investigations of spin-flip Raman scattering (SFRS) in GaAs/AlGaAs [1-3] and in CdMnTe/CdMgTe [4] multiple quantum wells provide useful information on the problems of exchange interaction and localization of two-dimensional excitons. The g factors of localized two-dimensional excitons and acceptor-bound heavy- and light-holes have been found. Experiments carried out in a tilted magnetic field led the authors of Ref. [3] to determine the anisotropy of the heavy-hole g factor and to measure independently the electron g factor. Exciton localization was shown to be crucial for the observation of SFRS [1-3].

Contrary to the one- and two-dimensional cases, complete exciton localization can be achieved in zero-dimensional systems. Attractive candidates for studies of SFRS in such quantum dots are structures with monolayer- (ML) and submonolayer InAs insertions in a GaAs matrix. Recently, equilibrium arrays of strained islands with equal size were shown to exist [5-8]. It has been demonstrated by using optical methods [6], and imaged directly in scanning tunneling microscopy studies [7], that the deposition of a small fraction of an InAs monolayer on (001)-oriented or vicinal GaAs surfaces results in spontaneous formation of InAs islands with a height of one monolayer and a uniform width of about 40Å. These islands are elongated in the $[\bar{1}10]$ direction and their length-to-width ratio changes from ~2 to ~4 for submonolayer structures with average InAs layer thicknesses of 1/6ML and 1/3ML, respectively. It is important to note that the average island separation for, e.g., 1/6 ML InAs is close to ~200Å, hence, larger than the GaAs exciton Bohr radius [9]. Thus, the InAs islands may be considered as uncoupled quantum dots in view of the lateral sizes involved. Another approach is to treat the submonolayer structures as systems of weakly bound bulk-like excitons. Recent studies of the photoluminescence (PL) spectra of InAs excitons associated with heavy (HH) and light (LH) hole states have demonstrated large exciton oscillator strengths [10] and exciton binding energies [11] even for diluted InAs coverage, thereby supporting the quantum dot model.

In this paper we investigate the spin splittings of excitons in InAs/GaAs structures with average InAs layer thicknesses of 1, 1/3, 1/6 and 1/12ML. Raman lines observed under resonant excitation are interpreted as the flip of the angular momentum of a localized HH exciton which is an intermediate state in the scattering process. The Raman shift is equal to the magnetic splitting of the exciton and is proportional to the component of its g factor along the direction of an applied magnetic field. The longitudinal components of HH and LH exciton g factors are determined. A variation of these values with the average InAs layer thickness is observed. The anisotropy of the exciton g factor causes a strong dependence of the spin-flip Raman shift on the angle between the direction of the magnetic field and the growth axes of the structure.

*) on leave from A.F. Ioffe Physical Technical Institute, Russian Academy of Sciences, 194021 St. Petersburg, Russia

EXPERIMENTAL

Samples with average InAs thicknesses of 1, 1/3, 1/6 and 1/12ML were grown by conventional solid source molecular-beam epitaxy on (001)-oriented GaAs semi-insulating substrates. Each sample contains one InAs layer confined between 2000Å of GaAs. This structure is surrounded by 6-periods of a (25Å/25Å) $GaAs/Al_{0.4}Ga_{0.6}As$ superlattice grown in order to trap impurities, to prevent surface recombination and to avoid surface-related electric fields. The growth rate was calibrated by the reflection high-energy electron diffraction technique and was equal to 0.1ML/s for InAs and to 1ML/s for GaAs. The background impurity concentration (mainly carbon) was below 10^{14} cm^{-3}, as it is manifested by the high mobility of two-dimensional electrons (around 10^6 $cm^2/(V \cdot s)$ at 4K) in modulation doped GaAs/AlGaAs structures grown under similar conditions. The procedure for the growth of InAs monolayer and submonolayer structures is discussed in detail in Refs. [6-8, 10].

The samples were mounted in an optical exchange-gas He-cryostat at a temperature of 5K. The SFRS experiments were carried out in magnetic fields (B) up to 14 T. A tunable Ti-sapphire laser pumped by an Ar^+-ion laser was used for PL and SFRS excitation . The pumping power was kept well below 0.1 W/cm^2 to avoid heating of the sample with the incident light and to improve the ratio between the Raman signal and the PL background. The PL and scattered light were analyzed by a SPEX 1404 double monochromator equipped with a cooled GaAs photomultiplier. The propagation direction of incident and scattered light was parallel to the magnetic field. Both, circularly and linearly polarized light was used for Raman and PL excitation and signal detection.

To describe the circular polarization of SFRS spectra we use the notation $z(\sigma^{\eta}, \sigma^{\lambda})\bar{z}$ where z and $\bar{z}$ correspond to the propagation direction of incident and scattered light, respectively. The circular polarizations of the exciting (σ^{η}) and scattered (σ^{λ}) photons are denoted by $\eta, \lambda = \pm$, respectively. The sign of η, λ is determined by the projection of the photon angular momentum on the z direction.

RESULTS

The PL spectra of the four samples used for the spin-splitting measurements are dominated by the InAs associated HH and LH exciton luminescence. InAs submonolayer insertions result in remarkably narrow exciton lines at energies between the values expected for a uniform 1ML InAs layer and the GaAs free exciton. The HH exciton energy is shifted to lower energies with respect to the position expected for a uniform 1ML-thick InGaAs layer with the same average In composition [10,11]. The optical orientation of the electron spin [12] in HH and LH excitons at B=0 enables us to determine unambiguously the symmetry of the hole states associated with them . The energy and the full width at half maximum (FWHM) of HH and LH exciton lines, already studied in [10,11], are presented in Table 1. In each sample PL features associated with the GaAs matrix are observed near the direct band gap.

Figure 1(a) shows the PL spectrum of the 1/6ML sample excited with a photon energy above the GaAs band gap in a magnetic field of B=10T directed perpendicular to the structure plane. In the magnetic field HH and LH exciton lines are split into two components with opposite circular polarization. The respective polarization is indicated on the figure with symbols σ^+ and σ^-. The peak separation (dE) increases directly proportional to the magnetic field.

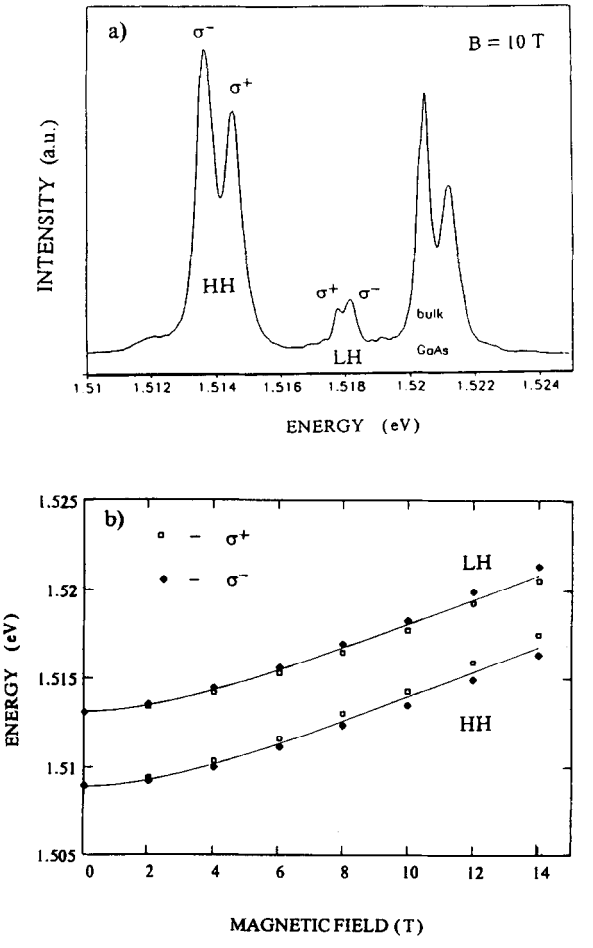

Fig.1 a) Photoluminescence spectrum of the 1/6ML InAs/GaAs sample in $z(\sigma^+,\sigma^- + \sigma^+)\bar{z}$ configuration at B=10T and T= 4K taken at an excitation energy of 1.65 eV. The labels HH and LH indicate heavy-hole and light-hole excitons associated with the InAs insertion. The features at 1.521 eV are related to band gap luminescence from the bulk GaAs matrix. The labels σ^+ and σ^- indicate the principal polarization of the magnetic field-split exciton peaks.

b) Energy of magnetic field-split HH and LH exciton peaks with σ^+ and σ^- polarization vs. magnetic field. The lines result from the fit to Eq.(1) with the parameters listed in Table 1.

Exciton localization energies derived from the dependence of the PL intensity on temperature are found to be several meV larger than the exciton FWHM. Detailed studies of the exciton localization in InAs/GaAs submonolayer structures are in progress.

Besides the paramagnetic splitting, the HH and LH exciton levels are also subject to a strong diamagnetic shift. Their peak positions (E) vs. B are shown in Fig.1(b) for the 1/6ML sample. The diamagnetic shift (E^{dm}) increases nonlinearly with B when the field is weaker than approximately 4T and linearly above 4T. The experimentally observed diamagnetic shift E^{dm} (E^{dm} = =E(B)–E(0)) of HH and LH excitons in the range of magnetic fields from 0 to 14T can be approximated by the expression:

$$E(B) = E_0 + \mu_0 B_0 \frac{m_0}{m^*} \cdot \sqrt{1+(B/B_0)^2} \qquad (1)$$

with the adjustable phenomenological parameters m^*/m_0, E_0 and B_0 listed in Table 1. The term describing the paramagnetic splitting is ignored in Eq. (1). The strong-field limit of this equation gives $E^{dm} \sim B$, while $E^{dm} \sim B^2$ in the weak-field limit. The parameter B_0 gives a characteristic field which corresponds to the boundary between weak- and strong-field regimes. The parameter B_0 decreases while m^*/m_0 increases with an increase in thickness of the InAs insertion. The values of B_0 and m^*/m_0 for the 1/12ML sample tend to the same bulk GaAs parameters as determined in Ref. [13] from D^oX-associated magneto-luminescence spectra.

For excitation in resonance with the HH exciton peak we observe narrow Stokes and anti-Stokes Raman lines. We confirmed that they follow the laser excitation energy when it is changed within the FWHM of the PL peak. Figure 2(a) shows a typical Stokes line, marked with the symbol *EX*, in the Raman spectrum for the 1/3ML sample measured at B=14T. These lines are strongly circularly polarized with the scattering efficiency of Stokes (anti-Stokes) processes being significant only in crossed $z(\sigma^+,\sigma^-)\bar{z}$ ($z(\sigma^-,\sigma^+)\bar{z}$) configuration when the energy of the exciting light coincides with the σ^+

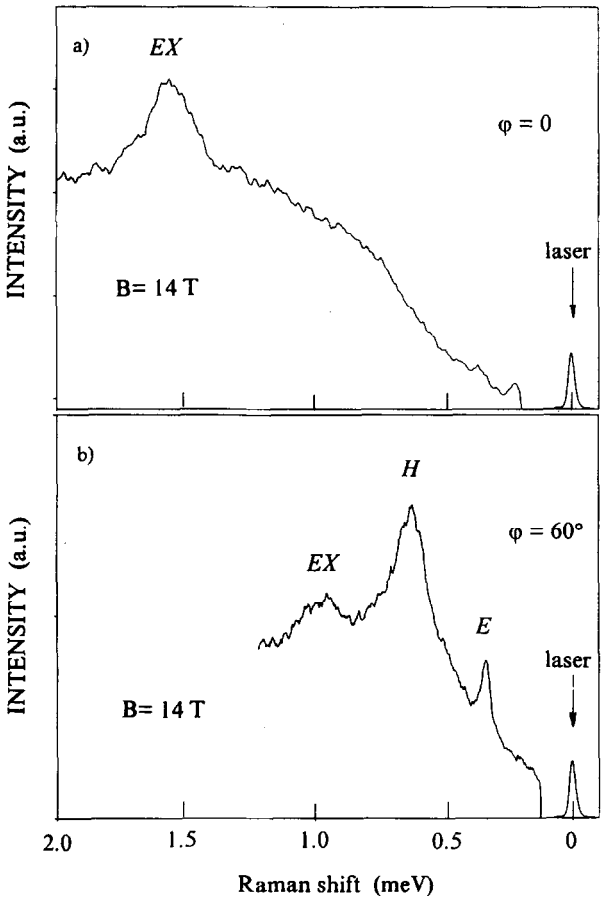

Fig.2 Raman spectra of the 1/3ML InAs/GaAs sample in $z(\sigma^+,\sigma^-)\bar{z}$ configuration at B=14T and T= 4K. The spectra were taken under resonant excitation of the σ^+ component of the HH exciton.

a) For angle between the magnetic field and the sample growth direction of φ= 0.

b) The same for φ= 60°.

The peaks marked as *EX*, *H* and *E* correspond to resonant SFRS between HH exciton states split in a magnetic field.

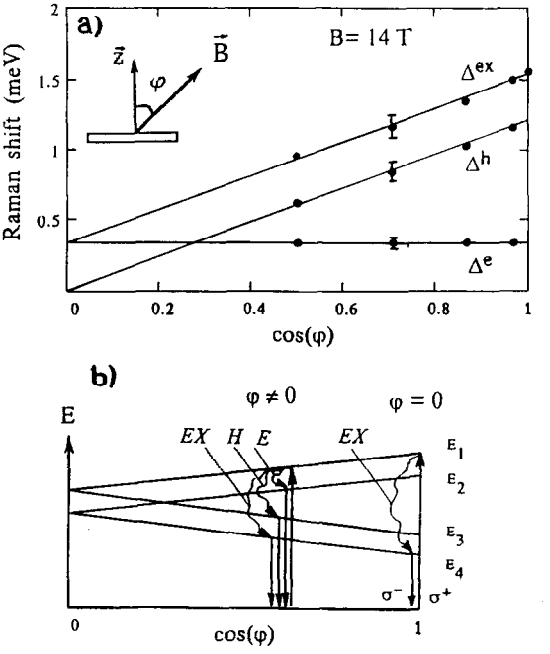

Fig.3 a) Raman shifts Δ^{ex}, Δ^h and Δ^e of the *EX*, *H* and *E* lines, respectively, vs. angle between the magnetic field and the sample growth direction for the 1/3ML InAs/GaAs sample at B=14T. The lines represent fits with $\Delta^h(\varphi)=\Delta^h(0)\cdot\cos\varphi$, Δ^e = Const and $\Delta^{ex}(\varphi)=\Delta^h(\varphi)+\Delta^e$.

b) Simplified scheme of SFRS processes in resonance with the E_1, E_2, E_3 and E_4 exciton states split in a magnetic field.

(σ^-) component of the HH exciton transition. They are absent in parallel $z(\sigma^+,\sigma^+)\bar{z}$ or $z(\sigma^-,\sigma^-)\bar{z}$ configurations. The Raman shifts (Δ^{ex}) of these lines are directly proportional to the magnetic field and coincide with the splitting dE determined from the PL measurements.

The Raman shift Δ^{ex} depends on the angle (φ) between the direction of the magnetic field and z. Figure 3(a) shows Δ^{ex} vs. cosφ for B=14T. We find that Δ^{ex} varies linearly with cosφ.

In a tilted magnetic field two new Raman lines appear with Stokes shifts less than Δ^{ex}. The Raman spectrum for φ=60° is shown in Fig.2(b), where these new peaks are indicated with the symbols *E* and *H*. Line *H*, observed only in crossed configurations, reveals the same polarization features as the line *EX*. Line *E* is detected in both, crossed and parallel configurations. While line *E* is most pronounced in parallel polarizations for small φ, it shows up more strongly in the crossed ones as φ increases. The intensity ratio $I(\sigma^+,\sigma^+)/I(\sigma^+,\sigma^-)$ of this line is approximately equal to 1 for φ=60°.

Figure 3(a) displays the Raman shifts of the lines *H* and *E*, Δ^h and Δ^e, respectively, as a function of cosφ. Δ^h is well described by a cosine function: $\Delta^h(\varphi)=\Delta^h(0)\cos\varphi$. Δ^e does not depend on the angle φ and is equal to $\Delta^e = \Delta^{ex} - \Delta^h$ within the experimental accuracy. No in-plane anisotropy of Δ^{ex}, Δ^h and Δ^e is observed.

DISCUSSION

We interpret the observed splitting dE in the circularly polarized PL spectra as the magnetic splitting of dipole-allowed localized HH and LH exciton levels. In turn, the Raman lines *EX*, *H*, and *E* result from the double resonant acoustic-phonon scattering with energies which are equal to the Zeeman splittings of the HH exciton.

We shall first describe the energy levels of HH and LH exciton states for an applied magnetic field parallel to z. The states $|\, s\,,\, j\,>$, where s= ±1/2 is the spin of the electron, and j= ±3/2 (j= ±1/2) are the quasi-angular momentum indices of holes in HH (LH) excitons, respectively, are expected to be approximate exciton eigenstates for an applied field, which is supposed to be strong enough to break up the exchange interaction. In this case the exchange splitting of the fourfold degenerate exciton levels at B=0 (due to spin-dependent electron-hole exchange) is small compared to Zeeman splittings and can be disregarded here. The states with s+j = ±1 are optically allowed, giving purely $\sigma^\pm$ polarized transitions, and others are forbidden. The energies of four LH and four HH exciton states are:

		$\|\, s\,,\, j\,>$ for $\varphi = 0$	
	LH:		
E_4	$= -1/2(g^{lh} + g^e)\mu_0 B$	$\|-1/2, -1/2>$	(σ^-)
E_3	$= -1/2(g^{lh} - g^e)\mu_0 B$	$\|+1/2, -1/2>$	
E_2	$= 1/2(g^{lh} - g^e)\mu_0 B$	$\|-1/2, +1/2>$	
E_1	$= 1/2(g^{lh} + g^e)\mu_0 B$	$\|+1/2, +1/2>$	(σ^+)

Table 1. Parameters of InAs-related HH and LH excitons for four samples with different average thicknesses of the InAs insertion. Peak positions of HH and LH excitons are given for B=0. The phenomenological parameters m^*/m_0, E_0 and B_0 are used for the calculation of the experimentally observed diamagnetic shift according to Eq.(1). The *g* factors labeled with (*) are measured by SFRS and PL, the others by PL only.

		1/12ML	1/6ML	1/3ML	1ML
HH exciton (eV)		1.5123	1.5089	1.5004	1.464
LH exciton (eV)		1.5141	1.5131	1.5106	-
FWHM of HH exciton (meV)		0.3	0.8	2	7
E_0 (eV)	HH	1.5093	1.5061	1.4986	-
	LH	-	1.5101	-	-
m^*/m_0	HH	0.073	0.078	0.087	-
	LH	-	0.078	-	-
B_0 (T)	HH	3.83	3.77	2.70	-
	LH	-	4.05	-	-
g^{ex}	HH	1.2	1.4 (*)	1.9 (*)	1.8 (*)
	LH	−1.0	−1.0	−0.4	-
g^e		-	−0.40 (*)	−0.40 (*)	−0.4 (*)
$g_{\|\|}^{hh}$		-	1.0 (*)	1.5 (*)	1.4 (*)
$g_{\perp}^{hh}$		-	~0 (*)	~0 (*)	~0 (*)

HH :

$E_1 = 1/2(g^{hh} - g^e)\mu_0 B$ $|-1/2,+3/2>$ (σ^+)

$E_2 = 1/2(g^{hh} + g^e)\mu_0 B$ $|+1/2,+3/2>$

$E_3 = -1/2(g^{hh} + g^e)\mu_0 B$ $|-1/2,-3/2>$

$E_4 = -1/2(g^{hh} - g^e)\mu_0 B$ $|+1/2,-3/2>$ (σ^-)

The parameters g^e , g^{hh} and g^{lh} are the components of the electron, the heavy- and the light-hole g factor tensors along the field direction, and μ_0 is the Bohr magneton. Optical transitions to E_1 and E_4 are optically allowed while E_2 and E_3 are forbidden. The separation between the σ^+ - and σ^- -circularly polarized components of the exciton PL spectra (Fig.1(a)) is equal to $dE = E_1 - E_4 = g^{ex}\mu_0 B$, where g^{ex} is the exciton g factor equal to $g^{hh} - g^e$ ($g^{lh} + g^e$) for HH (LH) excitons, respectively.

From the PL spectra we estimate the localized exciton g factors for the samples with 1/3, 1/6 and 1/12ML InAs content. The sign of the HH and LH exciton g factors is determined by the polarization of the PL lines. The corresponding data are listed in the Table 1.

In analogy to Refs. [1,3] we assume that spin-flip Raman lines observed under resonant excitation result from a HH exciton angular momentum flip. It was shown that such SFRS can be described as a result of three virtual transitions:

1. A HH exciton ground state $|-1/2,+3/2>$ ($|+1/2,-3/2>$) is excited by absorbtion of the σ^+ (σ^-) polarized light.
2. An inversion of electron and hole spins in the exciton takes place via an interaction with acoustic phonons.
3. The exciton recombines with the emission of a scattered photon which is polarized oppositely to the polarization of the exciting photon. The Raman shift Δ^{ex} is equal to the paramagnetic splitting of the exciton and reflects the component of its g factor along the field direction: $\Delta^{ex} = |g^{ex}\mu_0 B|$.

This SFRS process is accompanied by the emission or absorption of an acoustic phonon [1,3]. This is allowed if the exciton localization is strong enough for the relaxation of the crystal-momentum conservation condition. The high purity of the structures makes rather unlikely impurity-related mechanisms of SFRS, discussed in detail in Refs. [1,3], and additionally underlines the importance of strong exciton localization in the Raman process studied.

The longitudinal components of the HH exciton g factor for the 1, 1/3 and 1/6ML samples measured by SFRS are presented in Table 1. The FWHM of the exciton SFRS line ($\delta\Delta^{ex}$) is equal to 0.2 meV at B=14T, which is noticeably wider than the spectral slit-width. $\delta\Delta^{ex}$ increases with increasing B, so that the ratio $\delta\Delta^{ex}/\Delta^{ex}$ is approximately independent of the magnetic field and is equal to ~0.1. This inhomogeneous broadening of the exciton SFRS line reflects the spread of the exciton g factor in our samples: $\delta\Delta^{ex}/\Delta^{ex} = \delta g^{ex}/g^{ex}$.

A tilted magnetic field mixes the spin states s= +1/2 and s= −1/2 of an electron in an exciton. Thus, all four HH exciton states become optically allowed for backscattering along the z direction and the resonant transitions between them can be detected. We conjecture that the lines H and E in Fig.2(b) correspond to doubly resonant acoustic-phonon scattering with energies equal to the Zeeman splittings of the heavy-hole (Δ^h) and electron (Δ^e) states in the HH exciton. These splittings are determined as follows: $\Delta^h = |g^{hh}\mu_0 B|$ and $\Delta^e = |g^e\mu_0 B|$. The longitudinal component ($g_\parallel^{hh}$) of the heavy-hole g factor increases with an increasing InAs content. The values of $g_\parallel^{hh}$ for the 1, 1/3 and 1/6ML samples are listed in Table 1. The positive sign of the HH exciton and hole g factors is determined by the polarization of the corresponding SFRS and PL lines. The angular dependence $\Delta^h(\varphi)$ in Fig.3 shows that the transverse g factor ($g_\perp^{hh}$) of the heavy-hole is negligibly small, as it should be for a state with an angular momentum projection of j= ±3/2 along the quantization axis. This anisotropy in the hole g factor is closely related to the splitting of HH and LH states which in our samples is caused by both confinement and strain due to lattice constant mismatch. In the case of InAs islands having one monolayer (3Å) height and ≈ 40Å width both effects are the strongest along the *growth direction*.

The contributions of both, anisotropic *in-plane* confinement and *lateral* strain are much weaker due to the essentially two-dimensional shape of the islands (their height is much smaller than the lateral size). Moreover, these effects act in the opposite directions and could partially compensate each other. This would explain why no in-plane anisotropy of the hole g factors was observed.

According to the selection rules for optical transitions the electron line E should be observed only in $(\sigma^\pm, \sigma^\pm)$ configuration. The fact that it is also detected in crossed configurations indicates that admixture of the heavy-hole (j= ±3/2) and light-hole (j= ±1/2) wave functions takes place. Considering that there is no deviation of the angular dependence of the heavy-hole g factor from a cosine function, we conclude what this admixture is relatively small.

The negative sign of the electron g factor corresponds to the experimental observation of larger splittings for excitons than heavy-holes: $\Delta^{ex} > \Delta^h$. The electron g factor g^e for the 1, 1/3 and 1/6ML samples is isotropic and equals −(0.40±0.02), close to the value for bulk GaAs [14]. This is expected, in the spirit of **k·p** perturbation theory, from the close proximity of the gaps and spin-orbit splittings of the confined InAs structures and those of bulk GaAs [15]. Moreover, the FWHM of the electron line is much smaller than that of the exciton and hole lines, and is limited by the laser linewidth. This can be attributed to the fact that the electron component of the exciton wavefunction is expanded mainly in the GaAs matrix, whereas the hole component is more localized and is affected by fluctuations in lateral extention of the InAs islands. A possible anisotropy of the electron g factor should arise from the interaction of the conduction band with the split heavy- and light-hole states [16]. The small value of the HH-LH splitting in our samples makes this anisotropy unobservable.

We emphasize that the values of g^{ex}, g^{hh} and g^e were determined independently. The expected relationship $g^{ex} = g^{hh} - g^e$ is experimentally confirmed for magnetic field between 5 and 14 T. This proves, that the exchange splitting of the HH exciton is small compared to Zeeman splittings in our measurements.

CONCLUSIONS

We have observed very efficient SFRS processes in resonance with the HH exciton ground state in submonolayer InAs/GaAs structures. The results reflect the strong localization of excitons bound to InAs islands. The exciton, electron and heavy-hole g factors are determined. It is found that the electron g factor reveals quasi three-dimensional behaviour while the observed anisotropy of the heavy-hole g factor corresponds to the reduced symmetry of the investigated system.

Acknowledgments - We are thankful to B. P. Zakharchenya, D. N. Mirlin and E. L. Ivchenko for useful discussions, and to V. F. Sapega and A. A. Kiselev for a critical reading of the manuscript. Thanks are due to M. Cardona for continued support, discussions and a careful reading of the manuscript. We also would like to thank H. Hirt and M. Siemers for technical assistance. This work has been supported in different parts by the Volkswagen Foundation, the Russian Foundation of Fundamental Investigations and by the International Science Foundation.

REFERENCES

[1] V. F. Sapega, M. Cardona, K. Ploog, E. L. Ivchenko, and D. N. Mirlin, *Phys. Rev.* **B 45**, 4320 (1992).

[2] D. N. Mirlin and A. A. Sirenko, *Fiz. Tverd. Tela Leningrad*, **34**, 205 (1992). [*Sov. Phys. Solid State*, **34**, 108 (1992)].

[3] V. F. Sapega, T. Ruf, M. Cardona, K. Ploog, E. L. Ivchenko, and D. N. Mirlin, *Phys. Rev.* **B 50**, 2510 (1994).

[4] J. Stühler, G. Schaack, M. Dahl, A. Waag, G. Landwehr, K. V. Kavokin, and I. A. Merkulov, *Phys. Rev. Lett.* **74**, 2567 (1995).

[5] J. Tersoff and R. M. Tromp, *Phys. Rev. Lett.* **70**, 2782, (1993).

[6] P. D. Wang, N. N. Ledentsov, C. M. Sotomayor Torres, P. S. Kop'ev , and V.M. Ustinov, *Appl. Phys. Lett.* **64**, 1526 (1994).

[7] V. Bressler-Hill, A. Lorke, S. Varma, P. M. Petroff, K. Pond, and W. H. Weinberg, *Phys. Rev.* **B 50**, 8479 (1994).

[8] N. N. Ledentsov, P. D. Wang, C. M. Sotomayor Torres, A. Yu. Egorov, M. V. Maximov, V. M. Ustinov, A. E. Zhukov, and P. S. Kop'ev, *Phys Rev.* **B 50**, 12171 (1994).

[9] Sadao Adachi, *J. Appl. Phys.* **58**(3), R1 (1985).

[10] M. V. Belousov, N. N. Ledentsov, M. V. Maximov, P. D. Wang, I. N. Yasievich, N. N. Faleev, I. A. Kozin, V. M. Ustinov, P. S. Kop'ev, and C. M. Sotomayor Torres, *Phys. Rev.* **B 51**, 14346 (1995).

[11] P. D. Wang, N. N. Ledentsov, C. M. Sotomayor Torres, I. N. Yassievich, A. Pakhomov, A. Yu. Egorov, P. S. Kop'ev, and V. M. Ustinov, *Phys. Rev.* **B 50**, 1604 (1994).

[12] M. I. Dyakonov and V. I. Perel, " Theory of optical spin orientation of electrons and nuclei in semiconductors ". Chapter 2 in *Optical Orientation*, edited by F. Meier and B. P. Zakharchenya, p. 11. North-Holland (1984).

[13] V. A. Karasyuk, D. G. S. Beckett, M. K. Nissen, A. Villemaire, T. W. Steiner, and M. L. W. Thewalt, *Phys. Rev.* **B 49**, 16381 (1994).

[14] A. M. White, I. Hinchliffe, P. J. Dean, and P. D. Greene , *Solid State Commun.* **10**, 497 (1972).

[15] M. Cardona, N. E. Christensen, and G. Fasol, *Phys. Rev.* **B 38**, 1806 (1988).

[16] E.L. Ivchenko and A.A. Kiselev, *Fiz. Tekh. Poluprovodn.* **26**, 1471 (1992). [*Sov. Phys. Semicond.* **26**, 827 (1992)].